EB2012-BHE-004

ANALYSIS OF COORDINATION AND NOVEL BLENDING STRATEGY BETWEEN FRICTION BRAKE SYSTEM AND ELECTRIC MOTORS

[1]Shyrokau, Barys, [2]Savitski, Dzmitry, [1]Wang, Danwei, [2]Ivanov, Valentin[*], [2]Augsburg, Klaus
[1]Nanyang Technological University, Singapore, [2]Ilmenau University of Technology, Germany

KEYWORDS – electric vehicle, control allocation, recuperation, hardware in the loop, subsystem coordination

ABSTRACT - There are various strategies of control demand distribution between frictional brake system and electric motors of an electric vehicle. However, influence of subsystem coordination on electric vehicle (EV) characteristics, such as stability of motion, braking performance, energy recuperation and energy losses, is still weak-investigated. Moreover, subsystem coordination depends strongly on dynamic performance of actuators and on the vehicle manoeuvre. The main research objective of the presented study is a simulation-based analysis of EV subsystem coordination under various driving manoeuvres. The engineering objective is a development and testing of the blending control strategy providing optimal EV characteristics.

The work introduces the control system, which provides the coordination between a friction brake system and electric motors, and includes three levels: PI controller of vehicle dynamics control and demand correction, optimization-based control allocation with actuator and tyre friction constraints, low-level PI/PID actuator control. The simulation analysis of the proposed control system has been carried out using the full vehicle simulator in IPG/Carmaker. Based on simulation analysis, the coordination weights for the control allocation were defined to reach optimal characteristics of vehicle motion and energy consumption / losses. The experimental investigation of proposed control system has been performed on the hardware-in-the-loop (HIL) test rig with the real friction brake system, emulators of electric motors and IPG/Carmaker vehicle simulator.

The modelling covers three typical types of vehicle motion: straight-line braking, braking-in-turn and lateral motion based on “Sine with Dwell” test. Evaluation criteria for vehicle dynamics and stability of motion are (i) the braking distance, (ii) the root mean square error (RMSE) of yaw rate and (iii) the RMSE of sideslip angle. The measures for energy consumption and power losses are (i) the total amount of recuperated energy and (ii) the tyre energy dissipation. These criteria are investigated in respect to the blended operation of the friction brake system and electric motors. Thereby, obtained results demonstrate an influence of each subsystem on stability of motion, braking performance, energy recuperation and energy losses. Two variants of subsystem coordination are investigated using HIL test rig and compared.

The first part of the article, having more theoretical significance, relates to coordination analysis and has been investigated by computational simulation. The second part of the paper covers the emulation of electric motors and vehicle dynamics and refers to an application of online optimization-based control allocation, which requires heavier computation time as compared with other techniques.

The results proposed in this study leads to a novel EV brake blending strategy based on optimal control allocation with different subsystem coordination.

TECHNICAL PAPER –A distinguishing feature of the brake system architecture for electric vehicles is that the braking can be realized through the separate or parallel operation of friction brakes and electric motors. This combination calls for various research problems related to the system blending, regenerative braking, integration with powertrain and chassis sub-systems, and so forth. Many of the listed subjects have been extensively studied in recent years. However, among other topics, a complex assessment of influence of combined friction/electric braking on the vehicle dynamics is still rare explored. A possible methodology for solving this research problem becomes a higher level uncertainty in the case of control on driving manoeuvres with distinct lateral and yaw dynamics. An analysis of recent studies has revealed only single examples of corresponding applications. In particular, *Sumiya and Fujimoto* proposed the integrated control on a regenerative braking system and active steering (1). *Hac, Doman and Oppenheimer* researched the cooperative operation of brake-by-wire (BBW) and steer-by-wire for yaw dynamics control (2). *Jonasson and his colleagues* investigated the operation of different combinations of chassis subsystems embedded into the autonomous corner module including BBW, active suspension, steering and individual wheel drive (3, 4).

The presented paper introduces results of the study on benefits that can be achieved both for longitudinal and lateral vehicle dynamics by the coordinated control on friction brakes and electric motors. Despite the consideration of limited number of cooperated sub-systems, this variant of integration can still open new interesting technological solutions, for example, the recuperation of the vehicle energy released not only at braking but also at different turning manoeuvres. It should be mentioned that a relevant control strategy realizing the optimal blending between friction brakes and electric braking requires is a fairly complex task requiring simultaneous consideration the vehicle power balance, the cornering dynamics, the recuperation processes, and dynamics of the powertrain and brake actuators. The presented article discusses how the relevant control strategy can be realized with the use of control allocation methods.

Based on the results of previous and running research works, the authors of this paper have implemented the control allocation technique introduced in (5, 6). First of all, this approach is characterized by the multi-objective formulation of independent cost functions in terms of vehicle stability and energy consumption/power losses. The composition of cost functions is based on a set of diverse indicators as the braking distance, yaw rate, sideslip angle, recuperated energy, and tyre energy dissipation. Next sections of the article will illustrate how the proposed method can be applied to the development of the brake blending control strategy targeting optimal performance characteristics of the electric vehicle. The realization of the developed control strategy will be illustrated both with simulation and HIL experiments.

BRAKE CONTROL ARCHITECTURE OF ELECTRIC VEHICLE

The controller design, results of modelling and hardware tests presented in the study concern a full electric vehicle with all-wheel drive powertrain including individual electric motors for each wheel. Figure 1 displays the control architecture covering both the brake blending and vehicle dynamics control. The relevant configuration of the vehicle is as follows:

- Full mass 1534 kg;
- Tyres 205/55 R 16;
- Electric motors – in-board type; maximum power 20 kW; peak torque 50 Nm; maximum speed 14000 rpm;
- Friction brakes – hydraulic actuation; max. brake pressure 120 bar.

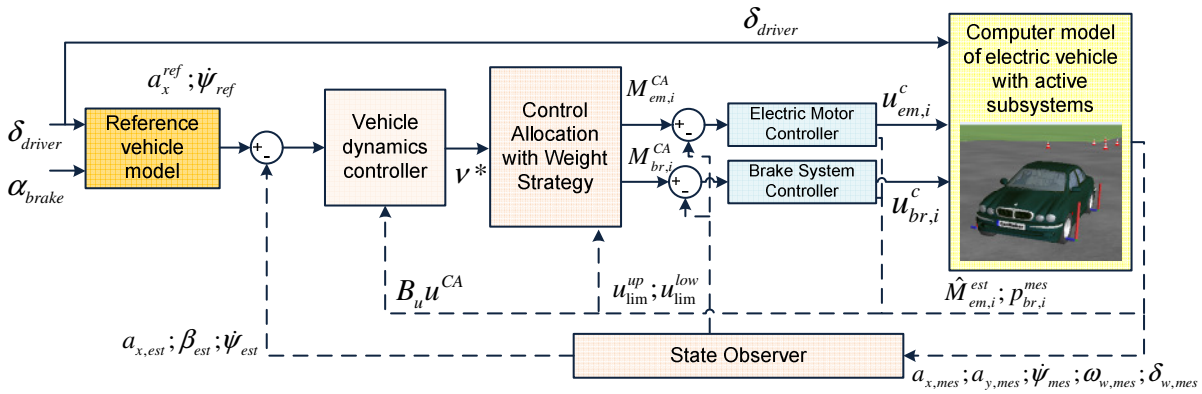

Figure 1: The control architecture

In accordance with Figure 1, the realization of the control strategy requires:

- Vehicle state estimator based on extended Kalman filter;
- High-level controller of vehicle motion;
- Middle-level control allocation;
- Lower-level individual controllers of each subsystem.

High-Level Control

The high-level control consists of reference vehicle model and vehicle dynamics controller. Generalized longitudinal and yaw torque are determined according to control errors. The reference longitudinal acceleration is calculated based on the measured pedal force:

$$a_x^{ref} = \begin{cases} -k_1 F_p - k_2, & a_x^{act} < a_x^{\max} \\ a_x^{\max}, & a_x^{act} \geq a_x^{\max} \end{cases}, \qquad (1)$$

where k_1 is the slope coefficient, kg^{-1}; k_2 is the initial deceleration caused by aerodynamic drag and rolling resistance, m/s^2; a_x^{max} is maximum acceleration constrained by friction limits, m/s^2; a_x^{act} is the actual deceleration, m/s^2.

For yaw rate the reference vehicle model is based on classical bicycle vehicle model. The reference yaw rate is constrained according to adhesion limits (7, 8).

The control demand is founded using PI controller:

$$\begin{cases} \nu_i = K_p e_i + K_i \int e_i dt \\ e_i = \begin{cases} a_x^{ref} - a_x^{mes}, & \left| a_x^{ref} - a_x^{mes} \right| > 0.1\ ms^{-2} \\ \dot{\psi}_{ref} - \dot{\psi}_{mes}, & \left| \dot{\psi}_{ref} - \dot{\psi}_{mes} \right| > 0.5^0\ s^{-1} \\ 0, & otherwise \end{cases} \end{cases} . \quad (2)$$

Control gains were selected using offline simulation-based optimization. The cost function is defined as minimization of RMS error of longitudinal acceleration and yaw rate. The gains are calculated as

$$\begin{aligned} K_p &= diag\left(\left[0.1m_a \quad 3I_{zz}\right]\right) \\ K_i &= diag\left(\left[m_a \quad 15I_{zz}\right]\right) \end{aligned} . \quad (3)$$

Middle-Level Control Allocation

The relationship between generalized lateral force and yaw torque from control demand and control inputs is nonlinear:

$$\nu_{HLdem} \approx \frac{\partial f(x, u_{k-1})}{\partial x} x + \frac{\partial f}{\partial u}\left(u_k - u_{k-1}\right) . \quad (4)$$

To compensate nonlinearity, the following correction of high-level demand is applied:

$$\nu^* = \nu_{HLdem} + \alpha B_u u_{k-1} , \quad (5)$$

where α is correction coefficient, $\alpha = diag([0.8\ 0.8])$.

To describe wheel dynamics in a braking mode, the coefficients ε_{Fxi} and η_{Fxi} are founded as (9):

$$\eta_{Fxi} = \frac{J_w V_{xw}}{C_{wxi} r_w t_s}; \quad \varepsilon_{Fxi} = \left(1 - \frac{r_w}{\eta_{Fxi}}\right) \hat{F}_{xwi} , \quad (6)$$

where the tyre longitudinal stiffness C_{wxi} is numerically computed from Pacejka model by Taylor series explanation with sampling time of *1ms*.

The control input vector is given as:

$$u^{CA} = \left[M_{em,i}^{CA,neg} \quad M_{br,i}^{CA} \right]^T . \quad (7)$$

The control effectiveness matrix B_u is equal to:

$$B_u = \left[B_{brake} \quad B_{emotor}^{neg} \right] . \quad (8)$$

Control effectiveness matrix for brake system B_{brake} can be written as follows:

$$B_{brake} = B_{emotor}^{neg} = \begin{bmatrix} \eta_{fl}^{-1} \cos\delta_{fl} & \eta_{fr}^{-1} \cos\delta_{fr} & \eta_{rl}^{-1} \cos\delta_{rl} & \eta_{rr}^{-1} \cos\delta_{rr} \\ B_x^{31} \eta_{fl}^{-1} & B_x^{32} \eta_{fr}^{-1} & B_x^{33} \eta_{rl}^{-1} & B_x^{34} \eta_{rr}^{-1} \end{bmatrix} (9)$$

$$B_x^{31} = -0.5 t_f \cos\delta_{fl} + a \sin\delta_{fl}; B_x^{32} = 0.5 t_f \cos\delta_{fr} + a \sin\delta_{fr};$$

$$B_x^{33} = -0.5 t_r \cos\delta_{rl} - b \sin\delta_{rl}; B_x^{34} = 0.5 t_r \cos\delta_{rr} - b \sin\delta_{rr};$$

The control allocation problem is formulated as a minimization of allocation error $(B_u u^{CA} - \nu^*)$ and control actuations u^{CA}, taking into account actuator constraints (10):

$$u_{CA} = \arg \min_{u_{\lim}^{low} \le u_{CA} \le u_{\lim}^{up}} \left(\left\| W_\nu (B_u u_{CA} - \nu^*) \right\|_2^2 + \zeta \left\| W_u u_{CA} \right\|_2^2 \right) . \quad (10)$$

The parameter ξ defines a significance of actuation minimization and equal to *0,2*. Matrix W_v is used to set up a priority among generalized longitudinal force and yaw torque. In this paper, lateral generalized force is neglected. Hence, W_v=*diag([1 1])*. The fixed-point method is applied to solve optimization problem. To provide blending between friction brake system and electric motors, weighting matrix W_u, which is related to restriction of control inputs, is used. The brake blending share (BBS) "brake/e-motor" belongs to the interval between 0 and 1. The weighted coefficients in the matrix W_u is defined as:

$$\begin{aligned} W_u^{brake} &= BBS \\ W_u^{emotor} &= 1 - BBS \end{aligned} \qquad (11)$$

Several limitations are related to longitudinal tyre forces for electric motor and friction brake system. It is assumed that tyre pressure variation has no strong impact and can be neglected for the tyre limitation. The limit of longitudinal force is calculated from the friction ellipse based on normal and lateral force, and friction coefficient. The actuator position and actuator rate limits are used as optimization constraints. Their values are shown on Table 1. The vehicle powertrain configuration has near-wheel motors. Hence, the rate limit of electric motor is less comparable with friction brake system due to low natural frequency of the haft-shafts.

Table 1- Position and rate limits of actuators

Subsystem	Position limit	Rate limit
Electric motor	Vary	5000 Nm/sec
Brake system	Vary	reduction / build-up 8000 / 12000 Nm/sec

Lower-Lever Actuator Control

Actuator control should achieve the following targets:
- guaranteeing precise tracking to reference control signals obtained from the middle level;
- estimation of boundary conditions for control allocation taking into account subsystem behaviour and skid/slip control.

Assuming that real torque of electric motor is precisely estimated, PWM signals are founded using PI motor control:

$$\begin{cases} u_{em,i}^c = K_p^{drive} e_{em,i} + K_i^{drive} \int e_{em,i} dt \\ e_{em,i} = M_{em,i}^{CA} - \hat{M}_{em,i}^{est} \end{cases}. \qquad (13)$$

Control signals for inlet and outlet valves of friction electro-hydraulic brake system are formulated as:

$$\begin{cases} u_{br,i}^c = K_p^{brake} e_{br,i} + K_i^{brake} \int e_{br,i} dt + K_d^{brake} \dfrac{de_{br,i}}{dt}; \\ e_{br,i} = p_{br,i}^{ref} - p_{br,i}^{mes} \end{cases}$$

$$u_{i,ideal}^{inlet} = \begin{cases} 1, & e_{br,i} \geq 0 \,\&\, \left|u_{br,i}^c\right| \geq 1 \\ \left|u_{br,i}^c\right|, & e_{br,i} \geq 0 \,\&\, \left|u_{br,i}^c\right| < 1 \\ 0, & e_{br,i} < 0 \end{cases}. \qquad (14)$$

$$u_{i,ideal}^{outlet} = \begin{cases} 0, & e_{br,i} \geq 0 \\ \left|u_{br,i}^c\right|, & e_{br,i} < 0 \,\&\, \left|u_{br,i}^c\right| < 1 \\ 1, & e_{br,i} < 0 \,\&\, \left|u_{br,i}^c\right| \geq 1 \end{cases}$$

The position limits of electric motors and brake system are varied to reach wheel skid/slip minimization and to correct limits according to the subsystem behaviour. For instance, torque limit of electric motor is corrected by weight coefficients, which are related to electric motor temperature, state-of-the-charge, longitudinal vehicle velocity, under and overvoltage protection and fault control (9):

$$M_i^{em,\lim} = f\left(u_{em,i}^c, w_m\right) \prod w_i \left(T_i, SOC, V_{xa}, U_i, fault\right). \quad (15)$$

The constructive parameters of brake mechanism and the level of wheel slip restrict the torque limit of friction brakes. The changing of torque limit depends on the threshold of wheel slip. The algorithm is rule-based slip control similar to traditional anti-lock brake system.

MODELS OF ELECTRIC VEHICLE AND SUB-SYSTEMS

Vehicle simulator

To investigate the electric vehicle dynamics, a vehicle simulator implemented in the IPG CarMaker software has been developed. The simulator allows integration of diverse mathematical and physical models of the vehicle and the vehicle systems within a unified software platform, for instance:

- Vehicle body - rigid model taking into account the mass distribution between wheel carriers, wheels, and body;
- Suspension - 2 DOF model of kinematics;
- Steering - static steer ratio model;
- Tyres - Pacejka Magic Formula model;
- Aerodynamics - 1D look-up table;
- Driver - user parameterized model defined by cruising speed, accelerations, and *g*-*g*-diagram;
- Road - numerical model of road geometry.

Two external user-defined Simulink models of the powertrain and the brake system were embedded into the vehicle simulator. Their short description is given in next sub-sections.

Model of electric powertrain

The simulated electric powertrain includes a battery and four in-wheel electric motors. The battery model has been composed in accordance with the Thevenin method (11). The model consists of an ideal no-load battery voltage, internal resistance, capacity and overvoltage resistance.

The electric motor model emulates both steady-state behaviour through a look-up table of motor characteristics and transient behaviour through the first-order transfer function with time delay (12). Figure 2 shows the torque-speed characteristic of the motor. Relevant partial characteristics are defined by the level of the pulse-width modulation duty obtained from the controller of the electric motor.

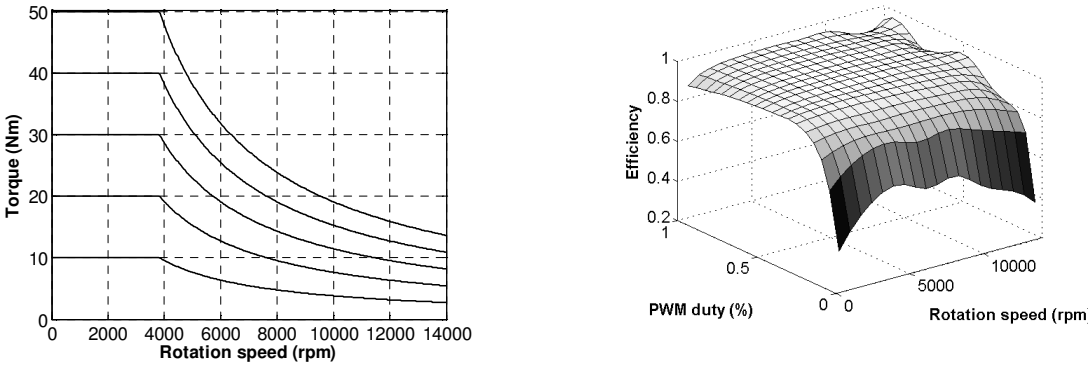

Figure 2 - Torque-speed and efficiency characteristics of the in-wheel motor (modified from (5))

The transient behaviour of the electric motor is described as:

$$T_{em,i} = \frac{T_{em,i}^{steady-state}}{\tau_m s + 1} e^{-t_d s}, \quad (16)$$

where $T_{em}^{steady\text{-}state}$ is the motor torque in steady-state conditions, τ_m and τ_d are time constants.

Model of brake system

The brake system has a typical electro-hydraulic layout, Figure 3. The reference pressure tracking is realized using the closed-loop control without taking into account delay effects caused by fluid inertia and brake line (5). The mathematical model of the hydraulic unit is based on the methodology proposed in (13).

The pump volumetric flow Q_{pump} depends on accumulator pressure and is represented by a look-up table. The control logic is defined as follows: switch-on of the pump by *p<160 bar*; switch-off of the pump by *p>180 bar*.

The volume change in the accumulator:

$$\dot{V}_{acc} = Q_{pump} - \sum_{i=1}^{4} Q_i \text{ , (17)}$$

where Q_i is the volumetric flow in the calliper. At that the volume changes in the i^{th} calliper can be found as:

$$\begin{aligned} \dot{V}_{bwci} &= Q_i + Q_j^{compensation} - Q_i^{dump} \qquad i = \{1,3\}; j = 1,2; \\ \dot{V}_{bwci} &= Q_i + Q_j^{block} - Q_j^{compensation} - Q_i^{dump} \qquad i = \{2,4\}; j = 1,2; \end{aligned}, \quad (18)$$

where indices "*block*", "*compensation*" and "*dump*" relate to the volumetric flows in the hydraulic block, the compensation valve and the dump valve correspondingly.

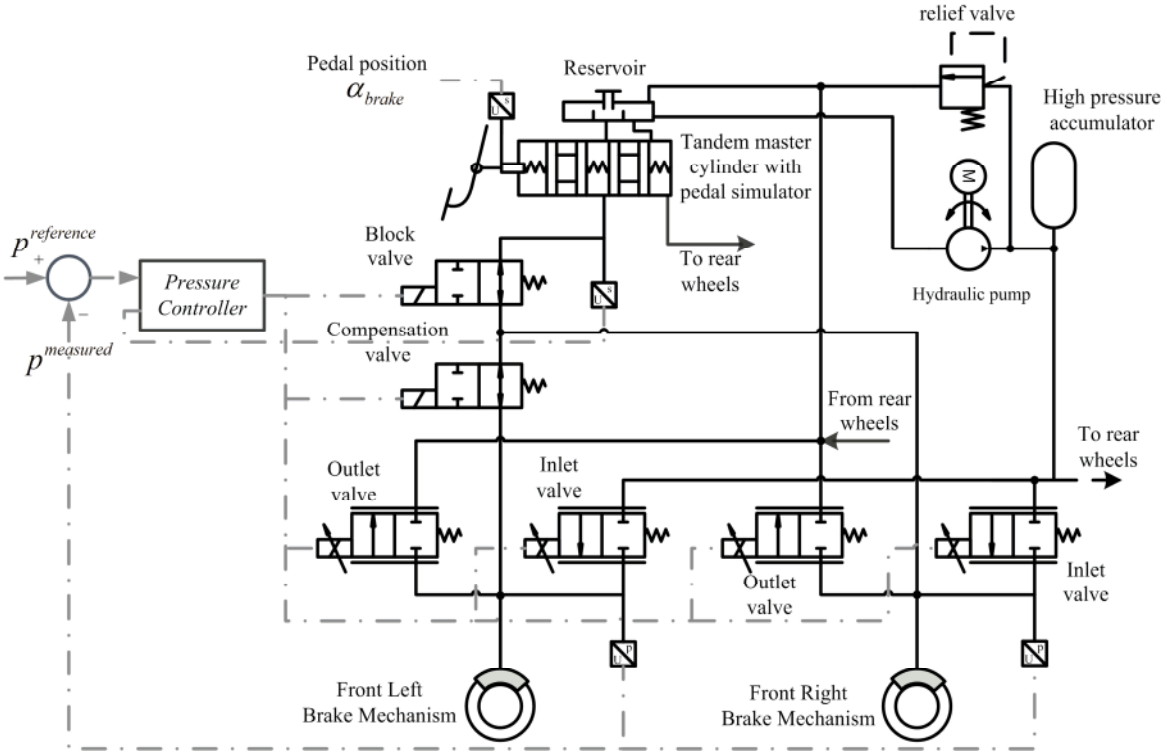

Figure 3 - Electro-hydraulic brake system (half view)

Due to typically short duration of braking processes, the accumulator can be described as an adiabatic process. The next assumption is that the gas pressure equals the fluid pressure at the accumulator inlet (14, 15). Pressure in the accumulator p_{acc} is calculated as:

$$p_{acc} = p_{acc,0}\left(\frac{V_{acc,0}}{V_{acc}}\right)^{\gamma} \text{ , (19)}$$

$$V_{acc} = V_{acc,0} - \int \dot{V}_{acc} dt \text{ . (20)}$$

The dynamics of valves are considered as a second-order transfer function (16, 17):

$$G_{valve}(s) = \frac{\omega_n^2}{s^2 + 2\xi\omega_n + \omega_n^2} \text{ . (21)}$$

The normal force generated by the calliper pressure between the brake pad and disk on each wheel is:

$$F_{ni} = \begin{cases} (p_i - p_0)\eta_c \dfrac{\pi d_{cyl}^2}{4}, & p_i > p_0 \\ 0, & p_i \le p_0 \end{cases} \text{ (22)}$$

Additional developed elements of the brake system model refer to dynamical friction coefficient and hysteresis of the brake system (18). They are not specified within the framework of this article.

ANALYSIS OF MODELLING RESULTS

Definition of case manoeuvres and criteria for performance evaluation

The evaluation of feasible effects that can be obtained through the implementation of the developed control strategy will be demonstrated by the example of three driving manoeuvres with the different complexity.

The first chosen manoeuvre is the straight-line braking defined for the initial vehicle velocity of 90 km/h. The assignment of the manoeuvre parameters in IPG CarMaker has been generally done in accordance with recommendations of the standard document DIN 70028 "Passenger Cars - Measuring the Stopping Distance with ABS in Straight-ahead Stops". The driver model follows the open-loop procedures for the directional control. This kind of test allows to assess pure longitudinal dynamics of the vehicle at braking.

The second test procedure is the "Sine with Dwell" defined by UN ECE Regulation 13H. By this test, the vehicle reaches firstly a velocity about 90 km/h (no steering or braking operation), after that the driving continues, and then a steering control takes place to shape a waveform of specially appointed geometry. The "sine with dwell" test is useful for estimation of the performance of automotive control systems from viewpoint of parameters of lateral dynamics.

The additional manoeuvre "Braking in a turn" was specifically chosen to test the control strategy in conditions of the vehicle motion with distinct lateral dynamics under the braking influence. Using the recommendations of the standard document ISO 7975 "Passenger cars - Braking in a turn - Open-loop test method", the testing procedure was implemented during the simulation as follows. The vehicle drives initially with a velocity of *90 km/h*. After *1* sec, the step steering angle is applied to generate lateral acceleration ~ *0.4 g*. After *4* sec, the vehicle decelerates with a reference deceleration ~ *0,45 g*.

The straight-line braking and the "sine with dwell" manoeuvre were simulated for three types of road surface with the friction coefficients μ*=0,8, 0,55* and *0,3*. The modelling of the braking in a turn was performed for μ*=0,8* and μ*=0,55*.

A number of the following criteria, Table 2, have been identified for the performance evaluation of the developed control technique:

i. Braking distance, m;

ii. Root mean square error of longitudinal acceleration, m/s^2:

$$RMSEa_x = \sqrt{\frac{1}{\tau}\int_0^{\tau}\left(a_x^{ref} - a_x^{mes}\right)^2 dt} \quad , (23)$$

where τ is the manoeuvre duration, sec; a_x^{ref} is the reference longitudinal acceleration; a_x^{mes} is the measured longitudinal acceleration;

iii. Total regenerated energy, kJ:

$$E_{em}^{total} = 10^{-3}\sum_{i=1}^{4}\int_0^{\tau} P_{em,i}\,dt \quad , (24)$$

where $P_{em,}$ is the power of an electric motor; i is the index of a wheel;

iv. Total tyre energy dissipation, kJ:

$$E_{tyre}^{total} = 10^{-3}\sum_{i=1}^{4}\int_0^{\tau}\left(F_{xwi}V_{swxi} + F_{ywi}V_{swyi}\right)dt \quad , (25)$$

where F_{xwi} is the longitudinal tyre force; F_{ywi} is the lateral tyre force; V_{swxi} is the longitudinal slip velocity; V_{swyi} is the lateral slip velocity;

v. Root mean square error of yaw rate, deg/s:

$$RMSE\dot{\psi} = \sqrt{\frac{1}{\tau}\int_0^{\tau}\left(\dot{\psi}_{ref} - \dot{\psi}_{mes}\right)^2 dt} \quad , (26)$$

where $d\psi/dt_{ref}$ is the reference yaw rate; $d\psi/dt_{mes}$ is the measured yaw rate;

vi. Root mean square of sideslip angle, deg:

$$RMS\beta_{mes} = \sqrt{\frac{1}{\tau}\int_0^{\tau}\beta_{mes}^2 dt} \quad , (27)$$

where β_{mes} is the measured sideslip angle.

Table 2 - Performance criteria

No.	Criterium	Evaluated vehicle attribute	Evaluated maneuver
i.	Braking distance	Safety	Straight-line braking
ii.	Root mean square error of longitudinal acceleration	Safety	Straight-line braking
iii.	Total regenerated energy	Energy	Straight-line braking, sine with dwell, braking in a turn
iv.	Total tyre energy dissipation	Energy	Straight-line braking, sine with dwell, braking in a turn
v.	Root mean square error of yaw rate	Safety	Sine with dwell, braking in a turn
vi.	Root mean square of sideslip angle	Safety	Sine with dwell, braking in a turn

Modelling of straight-line braking

Figure 4 shows normalized performance criteria as the function of the brake blending share (*BBS*) "brake/e-motor" in accordance with Eq. (11). A simplified procedure of normalization of the performance criteria is done in accordance with the following principle:

$$x_{norm,i} = x_i / x_{\max} \quad , (28)$$

where x_i is the value of a criterium by the given brake blending share, x_{max} is maximum value of a criterium the whole range of possible *BBS* combinations. Maximal absolute values of performance criteria in accordance with Eq. (28) are given in Table 3.

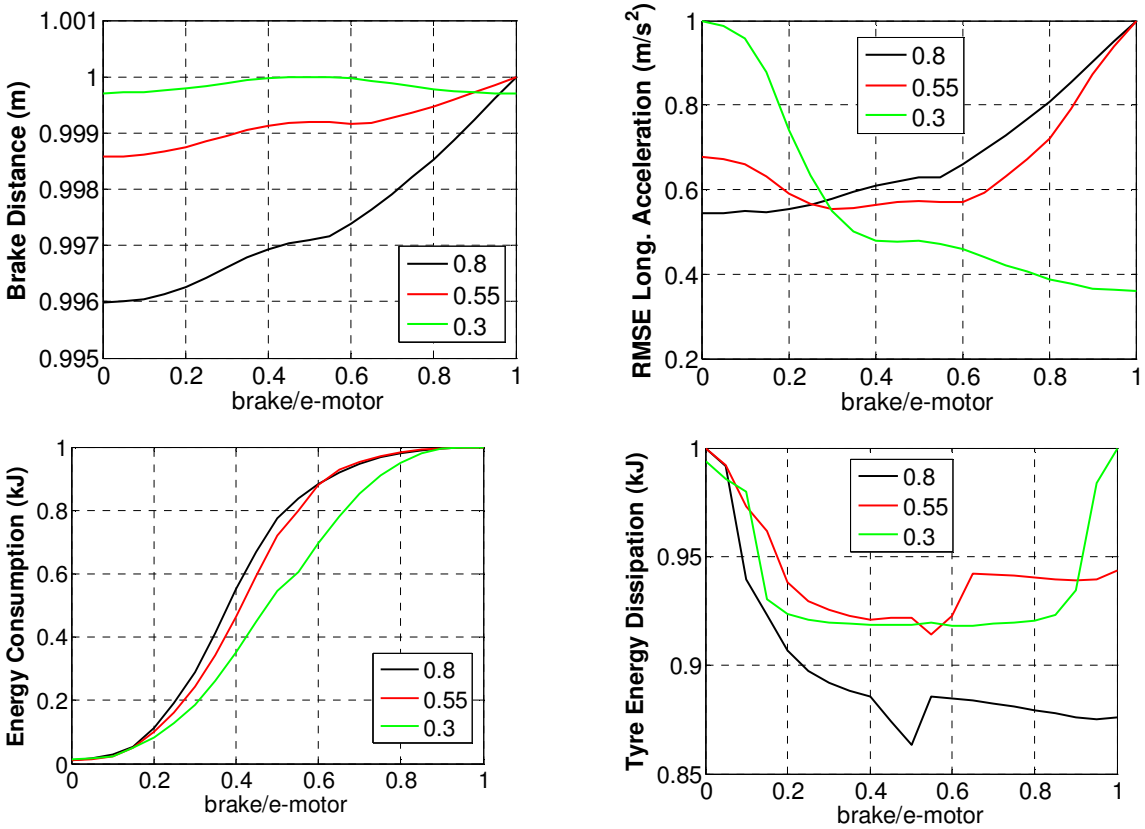

Figure 4 - Dependence of the normalized performance criteria from the *BBS* value at straight-line braking

Table 3 - Maximal values of performance criteria, straight-line braking

Criterium	μ=0,8	μ=0,55	μ=0,3
Braking distance, m	75,47	78,82	84,44
Root mean square error of longitudinal acceleration, m/s^2	0,18	0,07	0,04
Total regenerated energy, kJ (absolute value)	114,38	123,45	120,85
Total tyre energy dissipation, kJ	16,8	11,35	5,44

An analysis of Figures 4 allows to draw the following conclusions:

- Brake distance and, partially, tyre energy dissipation as performance criteria have no essential deviations depending on *BBS* therefore the weight factor for these criteria should be generally reduced;
- On the contrary, total energy consumption and *RMSE* of longitudinal acceleration are more sensitive indicators having a series of blending cases with the normalized deviation of *0,5* and more;
- All the performance indicators, excluding total energy consumption, are under appreciable influence of the friction coefficient; it can be especially recommended to rise a priority of *RMSE* of longitudinal acceleration for straight-line braking manoeuvres on surfaces with low friction.

Modelling of “Sine with Dwell” manoeuvre

By analogy with the previous modelling, Figure 5 displays the curves for performance criteria (see maximal value in Table 4) obtained from the simulation of the "Sine with Dwell" manoeuvre. An assessment of their behaviour leads to a number of observations:

- For given manoeuvre, criteria of power losses depend less from *BBS* value as compared with safety criteria. The one exception is the tyre energy dissipation for road conditions with high friction $\mu=0,8$. The optimal area for this parameter lies at $BBS<0,2$;
- *BBS* value has generally a noticeable influence on criteria of stability of motion, especially for *RMSE* of yaw rate;
- Both criteria of stability of motion - *RMSE* of yaw rate and *RMSE* of sideslip angle - shows quite different behaviour depending on the road friction; the partial or prevailing engagement of electric motors can be proposed for the manoeuvre on the low friction road.

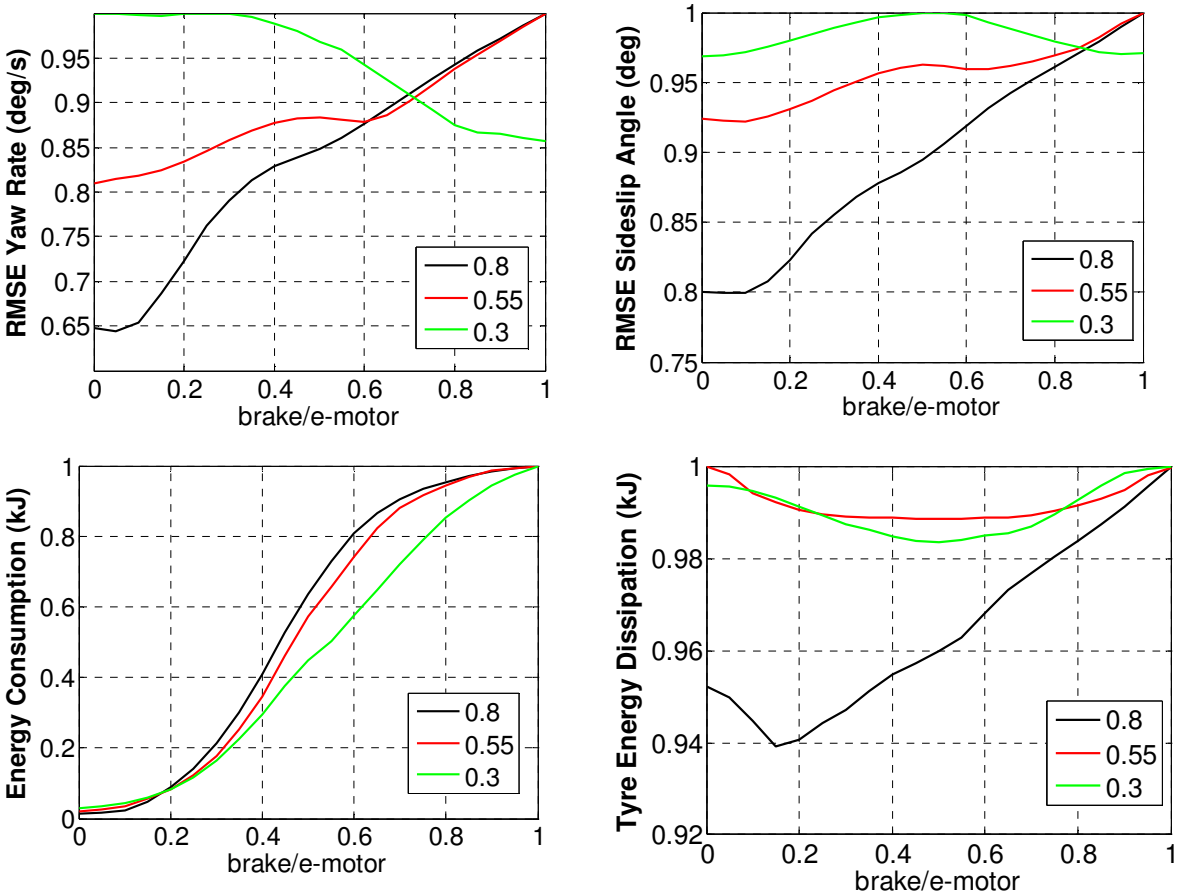

Figure 5 - Dependence of the normalized performance criteria from the brake blending share at "Sine with Dwell" manoeuvre

Table 4 - Maximal values of performance criteria, "Sine with Dwell" manoeuvre

Criterion	μ=0,8	μ=0,55	μ=0,3
Root mean square error of yaw rate, deg/s	3,67	2,38	1,53
Root mean square of sideslip angle, deg	0,94	0,5	0,26
Total regenerated energy, kJ (absolute value)	43,1	38,67	23,0
Total tyre energy dissipation, kJ	27,46	18,48	10,03

Modelling of braking in a turn

Figure 6 illustrates character of the performance criteria (see maximal value in Table 5) for the braking in a turn. This is a more complex manoeuvre as compared with two previous cases and therefore it is evaluated with six criteria. An analysis of the obtained results points to the following inferences:

- Magnitude of *BBS* exerts a less impact on the brake distance, the *RMSE* of sideslip angle as well as on the tyre energy dissipation (by middle level of the road friction). This observation correlates with the results of two manoeuvres discussed above. Other indicators are under considerable influence of *BBS*;
- Change of road friction calls for sensitive variations in behaviour of criteria of stability of motion and tyre energy dissipation that should be taken into account in deciding on the weighting factors.

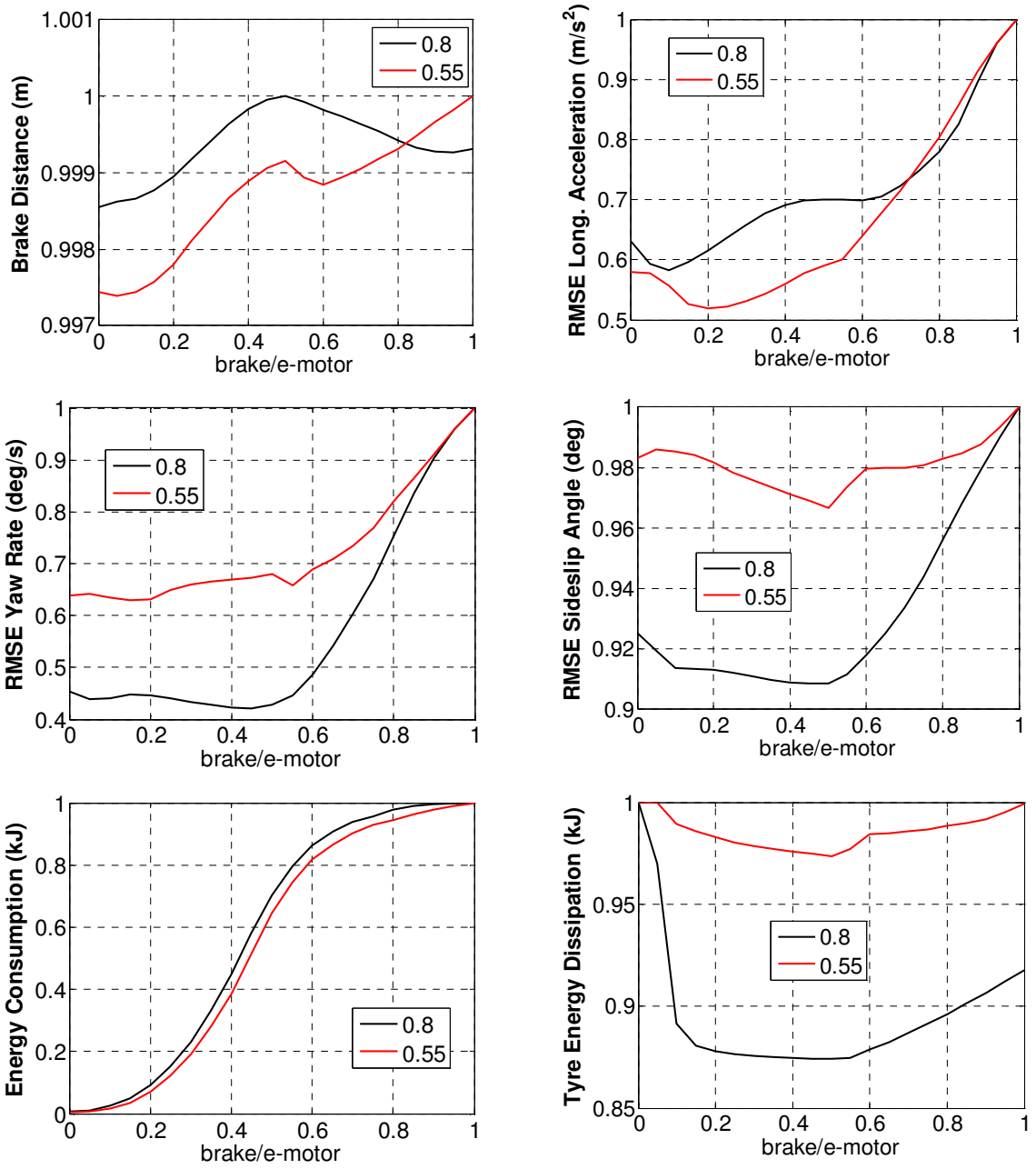

Figure 6 - Dependence of the normalized performance criteria from the brake blending share at braking in a turn

Table 5 - Maximal values of performance criteria, braking in a turn

Criterion	μ=0,8	μ=0,55
Braking distance, m	67,74	66,71
Root mean square error of longitudinal acceleration, m/s2	0,09	0,17
Root mean square error of yaw rate, deg/s	0,91	1,19
Root mean square of sideslip angle, deg	0,80	0,96
Total regenerated energy, kJ (absolute value)	124,25	100,2
Total tyre energy dissipation, kJ	26,15	27,72

Choice of optimal brake blending share

The modelling of three different manoeuvres discussed above confirms the complexity of the task of optimal choice of the brake blending share when an expedient compromise between vehicle stability and energy efficiency is required. For this purpose, the following basic method can be proposed:

1) Calculation of the cost function subset S_s from the performance indicators related to the vehicle stability:

$$S_s = \left\{ d_{norm}^{brake}; RMSE\dot{\psi}_{norm}; \frac{1}{3} d_{norm}^{brake} + \frac{2}{3} RMSE\dot{\psi}_{norm} \right\} \quad (29)$$

2) Calculation of the cost function subset S_e from the performance indicators related to the efficiency:

$$S_e = E_{em}^{total}{}_{norm} \quad (30)$$

3) Definition of the safety-based cost function J_1:

$$J_1 = w_{s1} \cdot S_s + w_{e1} \cdot S_e \,, \quad (31)$$

where w_{s1} and w_{e1} are the weighting factors.

4) Definition of the energy-based cost function J_2:

$$J_2 = w_{s2} \cdot S_s + w_{e2} \cdot S_e \,, \quad (32)$$

where w_{s2} and w_{e2} are the weighting factors.

5) Choice of the weighting factors is performed with the target to bring the cost functions to a dimensionless form in variables domain *[0, 1]*. This approach uses principles of formulation of cost functions for vehicle dynamics assessment introduced in (19). Within the framework of the presented study, it was appointed that w_{s1}*=0,9,* w_{e1}*=0,1,* w_{s2}*=0,1,* and w_{e2}*=0,9*.

6) The determination of an optimal value of the brake blending share is carried out as finding the trade-off between minimization of the cost function J_1 and maximization of the cost function J_2. Figure 7 gives a graphical representation of the determination procedure.

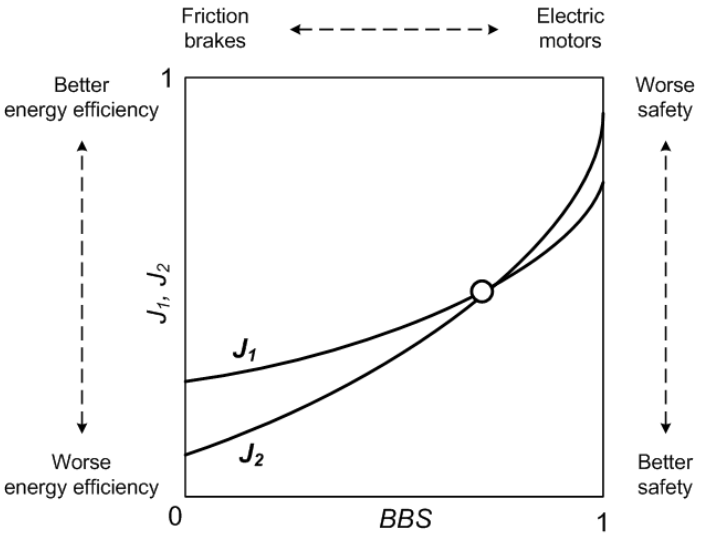

Figure 7 - Trade-off of cost functions

As applied to the simulated manoeuvres, Figure 8 introduces the results of calculation of integrated cost functions in accordance with Eqs. (31) and (32). An analysis of these results indicates that

- For the straight-line braking, there is a clear trade-off between cost functions of safety and energy: the trend of *BBS* to *1* is desirable from viewpoint of minimization of power losses but can negatively influence stability of vehicle motion. This conflict is true for all types of road surfaces and points toward optimal brake blending strategies avoiding generic friction/electric brake distributions.
- The recommended *BBS* area as applied to the straight-line braking belongs to *]0,8...0,9[*.
- For the "Sine with Dwell" manoeuvre, middle and high friction calls clearly for the brake blending with more involvement of conventional brakes to minimize the safety cost function.
- The recommended *BBS* area as applied to the "Sine with Dwell" manoeuvre belongs to *]0,65...0,8[*.
- The recommended *BBS* area as applied to the braking in a turn belongs to *]0,55...0,75[*.

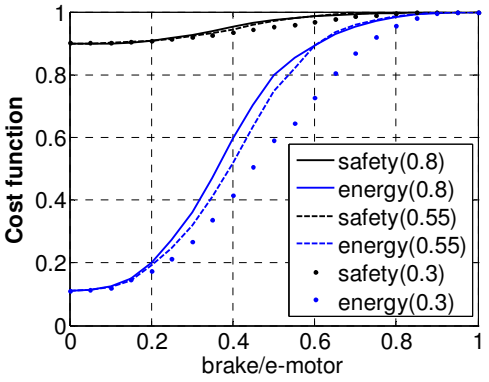

a)

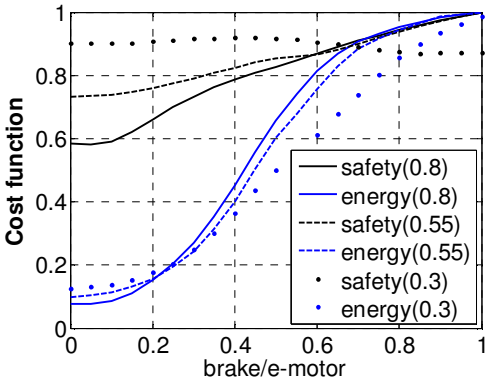

b)

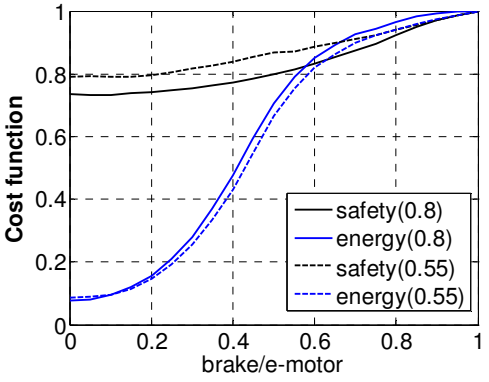

c)

Figure 8 – Cost functions as the function of the brake blending share for a) straight-line braking, b) "Sine with Dwell" manoeuvre, and c) braking in a turn
Legend:
"safety" – for cost function of J_1-type
"energy" – for cost function of J_2-type

Using the optimization procedure, the recommended brake blending value was chosen as *BBS=0,7*. The corresponding configuration of the brake control was a subject of hardware-based experiments introduced in next section.

ANALYSIS OF HIL TESTING RESULTS

Test rig description and definition of experimental programme

Experimental validation and assessment of the developed control strategy has been performed on the integrated hardware-in-the-loop test rig. This HIL test rig is realized on the flexible platform that provides plug-in adaptation of vehicle subsystems as additional modules (20). The platform, Figure 9, consists of real and virtual components, which are intercommunicated using hardware-in-the-loop technique. Hardware part is a conventional friction brake system, Figure 10. Other vehicle subsystems, including powertrain, multi-body vehicle model, and vehicle dynamics controller have software realization in MATLAB/Simulink and IPG CarMaker. The brake system has been equipped with two sensors mounted on the master cylinder to measure the pressure in the brake circuits and with four sensors mounted on each brake callipers to measure the pressure delivered to the wheel brake cylinders.

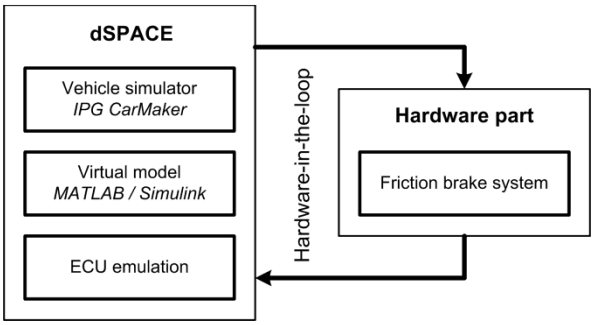

Figure 9 - HIL test rig scheme

Figure 10 - The physical configuration of the test rig

The experimental test programme has been defined in accordance with the following principles:

- Hardware-based analysis of the straight-line braking, "Sine with Dwell" manoeuvre and the braking in a turn, much as the simulation programme from the previous section "Analysis of Modelling Results";
- Test programme is limited by manoeuvre cases for the road surface with high level of friction only (μ=*0,8*);
- The brake system architecture is split into hardware part (conventional friction brake system) and emulated part (electric motors);
- Brake pressure in friction brake systems is generated by control settings of hydraulic pump;
- For the hardware part during the brake blending control, the reference brake torques are derived from the software model and the actual brake torques are computed using the real-time information from the pressure sensors installed on the test rig;
- For every test manoeuvre considered, two control configurations have to be investigated. The first configuration has a generic, neutral value of the brake blending share of *0,5*. The second configuration has an optimized *BBS* value of *0,7*: (*70%* for electric motors and *30%* for friction brakes).

Next sub-sections introduce outcomes of relevant HIL tests.

HIL tests of straight-line braking

The results of HIL tests of the vehicle simulator in straight-line braking are shown on Figure 11. These results are given for the optimized *BBS=0,7*. Table 6 compares results obtained for optimized and neutral *BBS* values.

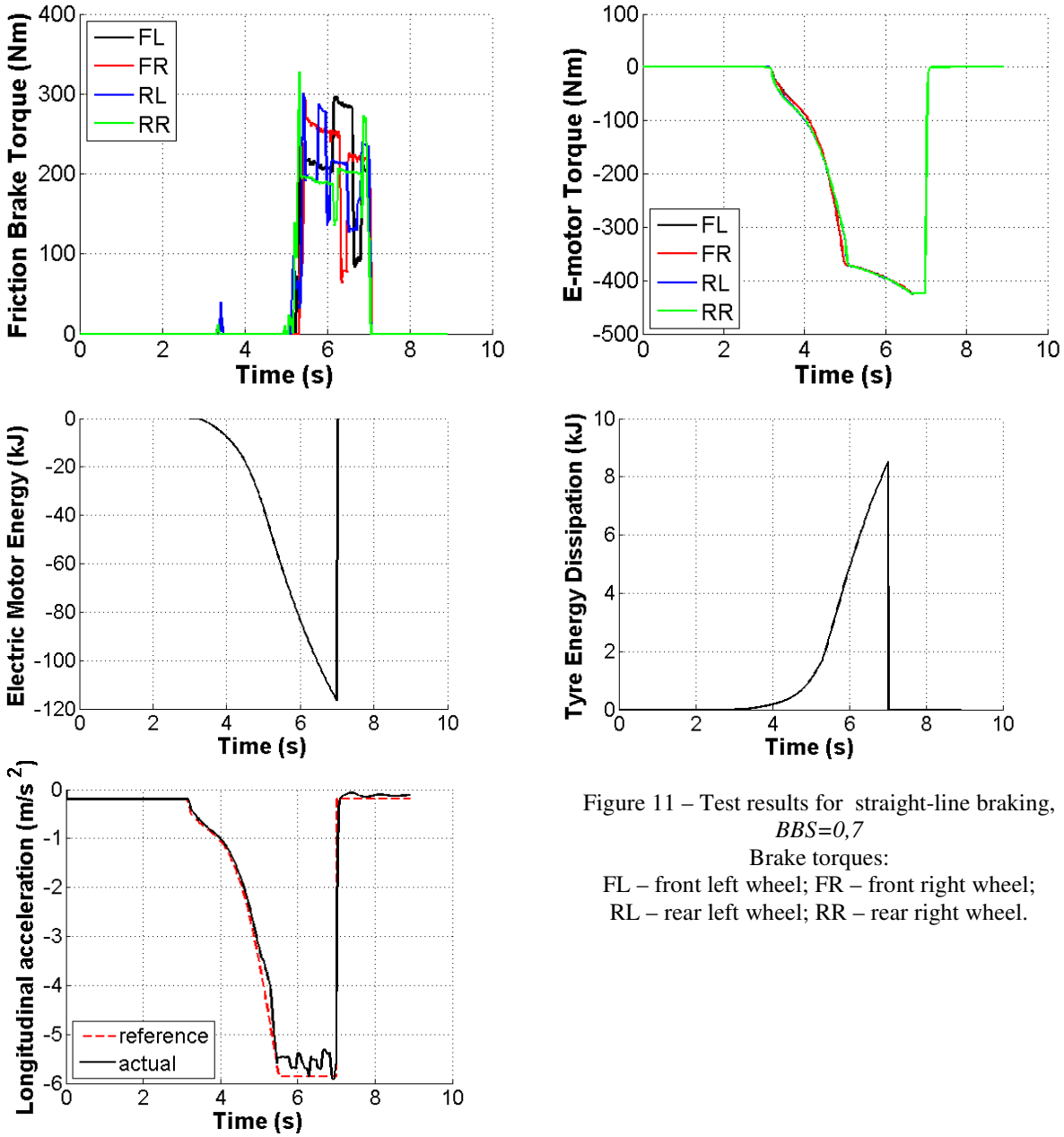

Figure 11 – Test results for straight-line braking, *BBS=0,7*
Brake torques:
FL – front left wheel; FR – front right wheel;
RL – rear left wheel; RR – rear right wheel.

Table 6 - Maximum values of performance criteria, braking in a turn

Criterium	BBS=0,7	BBS=0,5	Relative difference, % (specified to BBS=0,5)
Root mean square error of longitudinal acceleration, m/s^2	0,28	0,24	16,7
Total regenerated energy, kJ (absolute value)	116,7	98,59	18,4
Total tyre energy dissipation, kJ	8,51	8,3	2,5

Assessment of the test results can be summarized as follows:

- To follow appointed cost functions, the control on the system is organized through smooth growth of electric brake share and low-frequency modulation of pressure in the friction brake system;
- Inclusion of electric braking lasts about *4* sec reaching the level of *115 kJ* of energy that can be potentially recuperated;
- Maximum deviation between the reference and actual values of longitudinal acceleration was below *0,3* m/s^2 pointing to sufficient control quality;
- The strategy *BBS=0,7* provides a better energy consumption indictors as compared with the strategy *BBS=0,5*; the safety level is comparable for both strategies.

HIL tests of "Sine with Dwell" manoeuvre

The testing of “Sine with Dwell” manoeuvre can be assessed with the results given on Figure 12 and Table 7.

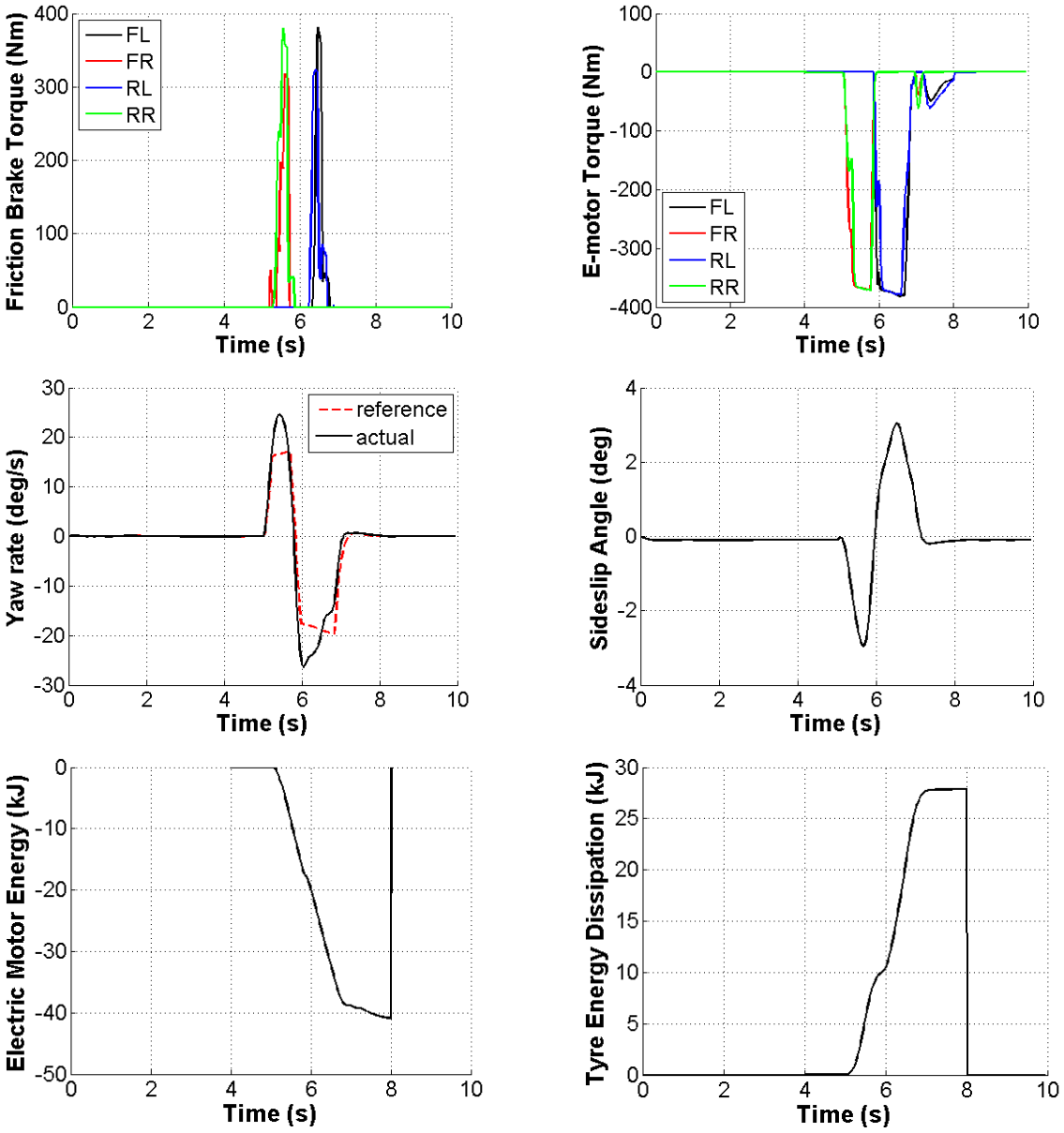

Figure 12 – Test results for “Sine with Dwell” manoeuvre, *BBS=0,7*
Brake torques: FL – front left wheel; FR – front right wheel; RL – rear left wheel; RR – rear right wheel

Table 7 - Maximum values of performance criteria, “Sine with Dwell” manoeuvre

Criterium	BBS=0,7	BBS=0,5	Relative difference, % (specified to BBS=0,5)
Root mean square error of yaw rate, deg/s	0,07	0,06	16,7
Root mean square of sideslip angle, deg	0,02	0,02	0,0
Total regenerated energy, kJ (absolute value)	38,85	28,65	35,6
Total tyre energy dissipation, kJ	27,69	27,39	1,1

An analysis of results allows to draw a number of conclusions:

- The proposed control strategy has properly combined blending of friction and electric brakes to keep the stability of the vehicle during the manoeuvre with distinct lateral dynamics; it can be shown that the brake blending can practically adopt the functions of an ordinary stability control system;
- The developed control allocation technique allowed a good tracking of reference yaw rate with small deviations *<7 deg/s*;
- The results point to a possibility to gain potentially recuperated energy during the traction manoeuvres with lateral dynamics control; despite minor amounts of this energy, this possibility should be considered for further technologies of regenerative systems.

HIL tests of braking in a turn

Figure 13 and Table 8 displays the experimental results for braking in a turn.

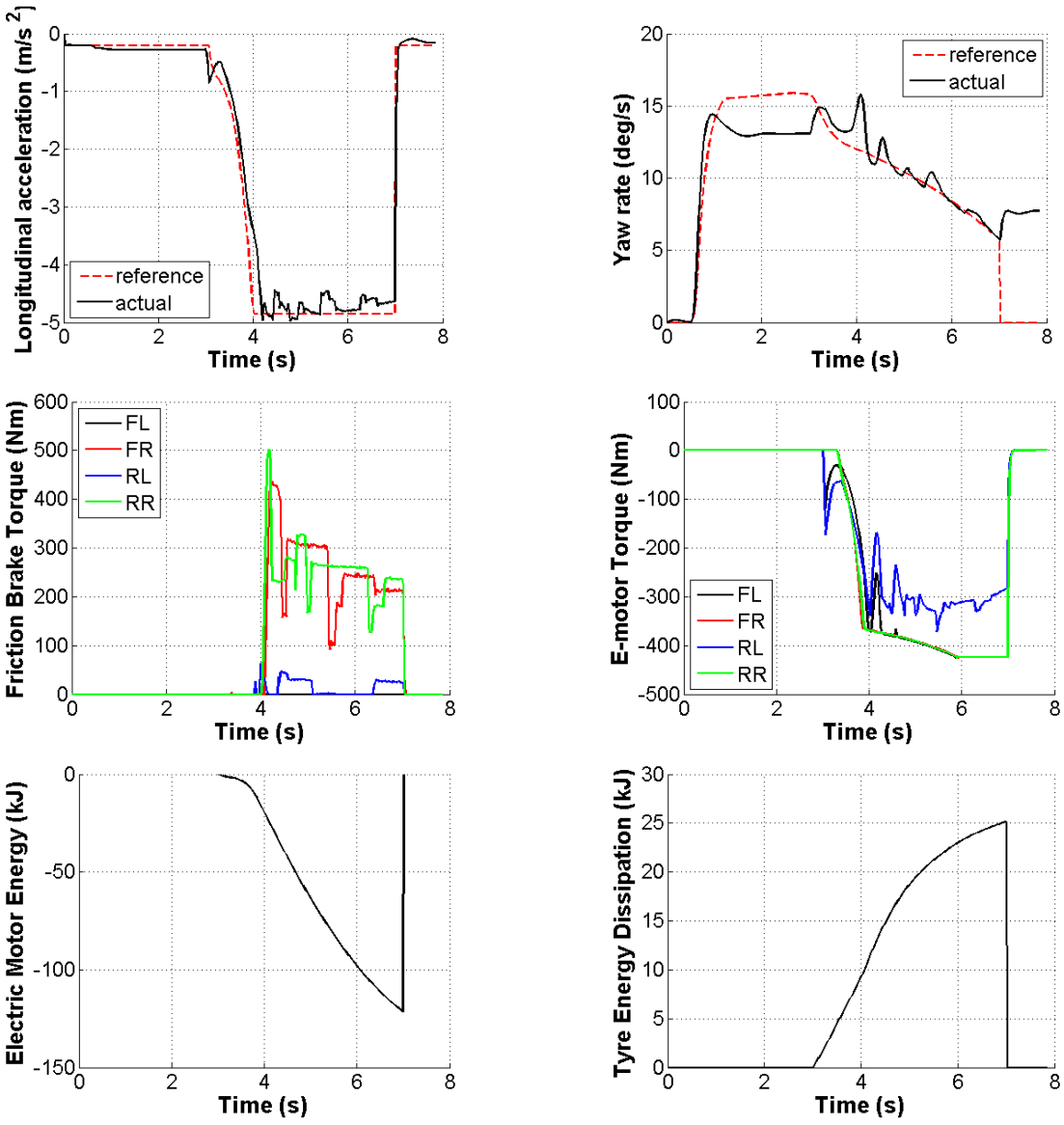

Figure 13 – Test results for braking in a turn, *BBS=0,7*

Brake torques: FL – front left wheel; FR – front right wheel; RL – rear left wheel; RR – rear right wheel

Table 8 - Maximum values of performance criteria, braking in a turn

Criterium	BBS=0,7	BBS=0,5	Relative difference, % (specified to BBS=0,5)
Root mean square error of longitudinal acceleration, m/s^2	0,36	0,31	16,1
Root mean square error of yaw rate, deg/s	0,02	0,01	100,0
Root mean square of sideslip angle, deg	0,02	0,02	0,0
Total regenerated energy, kJ (absolute value)	121,54	100,49	20,9
Total tyre energy dissipation, kJ	25,16	24,59	2,3

The following observations have been done for this manoeuvre:

- Both variants of brake blending with *BBS=0,7* and *BBS=0,5* provide similar level of performance indicators related to stability of vehicle motion; regarding the energy consumption, the control with *BBS=0,7* gives better results;
- The control technique guarantee a good tracing of reference dynamics in relation both to longitudinal acceleration (deviations *<0,3 m/s²*) and yaw rate (deviations *<3 deg/s*);
- The developed brake blending on the basis of control allocation shows proper distribution of friction and electric brakes as the combin[a]tion of board-related and axle-related control on individual wheels.

CONCLUSIONS

The presented work has introduced novel strategy for brake blending in an electric vehicle on the basis of control allocation technique. For this purpose, the weighted performance criteria for simultaneous evaluation of the vehicle stability and energy consumption have been developed and integrated as components of cost functions. This multi-objective formulation was supplemented with the procedure of definition of optimal blending share between the friction and electric brakes to find a better trade-off between the safety and energy factors.

The developed methodology was initially investigated with software-based vehicle simulator including detailed models of the hydraulic brake system and electric powertrain. The optimization of the brake blending share was carried out on the basis of the modelling of three different manoeuvres on surfaces with high, middle and low levels of the road friction. From the viewpoint of both longitudinal and lateral dynamics, an optimal value of the brake blending share *BBS=0,7* was proposed (*70%* for electric motors and *30%* for friction brakes). This variant was experimentally investigated using the hardware-in-the-loop technique with the real brake system and emulated electric propulsion system. The test results have confirmed good functionality of the developed system allowing to reach an effect in the energy recuperation simultaneously keeping of vehicle stability.

The control allocation technology presented in this study can be in further advanced for various tasks of integrated control of electric vehicle subsystems.

ACKNOWLEDGEMENTS

This work relates to the scientific activities of the research group PORT at Ilmenau University of Technology, and to the project IEV, funded by the European Regional Development Fund. This publication is made possible by the Singapore National Research Foundation under its Campus for Research Excellence And Technological Enterprise (CREATE) programme. The views expressed herein are solely the responsibility of the authors and do not necessarily represent the official views of the Foundation. It is also supported in part by National Natural Science Foundation of China (91120308).

REFERENCES

(1) Sumiya, H., and Fujimoto H., "Range extension control system for electric vehicle with active front steering and driving/braking force distribution on curving road", IECON Proceedings (Industrial Electronics Conference), art. no. 5674927, pp. 2352-2357, 2010.

(2) Hac, A., Doman, D., and Oppenheimer, M., "Unified Control of Brake- and Steer-by-Wire Systems Using Optimal Control Allocation Methods", SAE Technical Paper 2006-01-0924, 2006.

(3) Jonasson, M., and Wallmark, O., "Control of electric vehicles with autonomous corner modules: implementation aspects and fault handling", International Journal of Vehicle Systems Modelling and Testing, Vol. 3, Issue 3, pp. 213-228, 2008.

(4) Jonasson, M., Andreasson, J., Jacobson, B., and Trigell A.S., "Global force potential of over-actuated vehicles", Vehicle System Dynamics, Vol. 48, Issue 9, pp. 983-998, 2010.

(5) Shyrokau, B., Wang, D., Savitski, D., and Ivanov, V., "Vehicle Dynamics Control with Energy Recuperation based on Control Allocation for Independent Wheel Motors and Brake System", Int. Journal of Powertrains, 2012 (in press), http://www.inderscience.com/jhome.php?jcode=ijpt

(6) Shyrokau, B., and Wang, D., " Coordination of Steer Angles, Tyre Inflation Pressure, Brake and Drive Torques for Vehicle Dynamics Control", SAE Technical Paper 2013-01-0712, 2013.
(7) Dixon, J., "Tires, Suspension and Handling", Warrendale, PA, Society of Automotive Engineers, 1996.
(8) Rajamani, R., "Vehicle Dynamics and Control", Springer, New York, USA, 2005.
(9) Kou, Y., "Development and evaluation of integrated chassis control systems", PhD thesis, University of Michigan, 2010.
(10) Härkegård, O., "Backstepping and control allocation with applications to flight control", PhD thesis, Linköpings universitet, 2003.
(11) Chan, H. L,. and Sutanto, D., "A new battery model for use with battery energy storage systems and electric vehicles power systems", Proc. of IEEE PES Winter Meeting, pp. 470–475, 2000.
(12) Wang, B., Wang, R., Hanwen, S., and Qunying, C., "Simulation research on vehicle stability control for 4WD electric vehicle", in Proc . of the 3rd International Conference on Measuring Technology and Mechatronics Automation, Shanghai, China, pp. 274-277, 2011.
(13) Kuang, M., Fodor, M., and Hrovat, D., "Hydraulic brake system modeling and control for active control of vehicle dynamics", Proc. of American Control Conference (ACC), San Diego, Califonia, USA, pp. 538-542, 1999.
(14) Midgley, W., and Cebon, D., "Specifying a hydraulic regenerative braking system for an articulated urban delivery vehicle", Proc. of IEEE Vehicle Power and Propulsion Conference, Chicago, Illinois, USA, 2011, pp. 1-6, 2011.
(15) Ho, T.H., and Ahn, K.K. "Speed control of a hydraulic pressure coupling drive using an adaptive fuzzy sliding-mode control", IEEE/ASME Transactions on Mechatronics, Vol. 17, No. 5, pp. 976 - 986, 2011.
(16) Altintas, Y., and Lane, A.J., "Design of an electro-hydraulic CNC press brake", International Journal of Machine Tools and Manufacture, Vol. 37, pp. 45-59, 1997.
(17) Kazemi, R., and Zaviyeh, K.J., "Development of a new ABS for passenger cars using dynamic surface control method", in Proc. of American Control Conference (ACC), Arlington, Virginia, USA, pp. 677-683, 2001.
(18) Shyrokau, B., Wang, D., Augsburg, K., and Ivanov, V., "Vehicle dynamics with brake hysteresis", Proc. of the IMechE, Part D: Journal of Automobile Engineering, Vol. 227, No. 2, pp. 139-150, 2013.
(19) Savitski, D., Plihal, J., Nedoma, P., Machan, J., Ivanov, V., and Augsburg, K., "Cost Functions for Assessment of Vehicle Dynamics", Proc. of 2013 IEEE Symposium Series on Computational Intelligence, Singapore, 2013.
(20) Heidrich, L., Shyrokau, B., Savitski, D., Ivanov, V., Augsburg, K., and Wang, D., "Hardware-in-the-loop test rig for integrated vehicle control systems", Proc. of the 7th IFAC Symposium of Advances in Automotive Control, Tokyo, Japan, 2013 (in press).